Atmospheric Environment 360 (2025) 121347

Contents lists available at ScienceDirect

Atmospheric Environment

journal homepage: www.elsevier.com/locate/atmosenv

Assessing the efficiency of different mitigation strategies to reduce shipping related air pollution levels and exposure in the Mediterranean coastal region – An ensemble modelling approach

Evangelia Fragkou [a,*], George Tsegas [b], Ummugulsum Alyuz [c], Risto Hänninen [d], Jana Moldanova [e], Sara Jutterström [e], Elisa Majamäki [d], Jukka-Pekka Jalkanen [d], Ranjeet S. Sokhi [c], Jaakko Kukkonen [d], Mikhail Sofiev [d], Leonidas Ntziachristos [a]

[a] *Laboratory of Applied Thermodynamics, School of Mechanical Engineering, Aristotle University of Thessaloniki, Thessaloniki, 541 24, Greece*
[b] *Sustainability Engineering Laboratory, School of Mechanical Engineering, Aristotle University of Thessaloniki, Thessaloniki, 541 24, Greece*
[c] *Centre for Climate Change Research (C3R), School of Physics, Engineering and Computer Science, University of Hertfordshire, College Lane, Hatfield, AL10 9AB, UK*
[d] *Atmospheric Composition, Finnish Meteorological Institute, Erik Palmen's Square 1, 005 60, Helsinki, Finland*
[e] *IVL Swedish Environmental Research Institute, Box 530 21, 400 14, Gothenburg, Sweden*

HIGHLIGHTS

- Detailed updated shipping emissions are used to evaluate future policy scenarios.
- Ensemble means of three chemical transport models are calculated for scenario analysis.
- Population weighted concentrations in 30 Mediterranean coastal cities are produced.

ARTICLE INFO

Keywords:
Shipping emissions
Mediterranean air quality
Shipping emission reduction scenarios
Population weighted exposure
Air quality management
Scrubbers

ABSTRACT

The air quality in the Mediterranean coastal region is adversely affected by rising shipping emissions in the area. The present study demonstrates the results of an ensemble modelling approach for assessing the impact of shipping emissions on current and future air quality concentrations and exposure in the coastal Mediterranean region.

Ensemble model means were calculated based on the results of three regional or global dispersion models (EMEP, SILAM and CMAQ) to simulate annual and seasonal atmospheric pollutant dispersion patterns in the Mediterranean region, under the baseline 2018 scenario and two 2050 future scenarios developed within the EMERGE (Evaluation, control and Mitigation of the EnviRonmental impacts of shippinG Emissions) project. The selected scenarios examine the impact of a) the designation of a Mediterranean Sulfur/Nitrogen Emission Control Area (SECA/NECA) and the extensive use of open-loop scrubbers, Exhaust Gas Cleaning Systems and Selective Catalytic Reduction systems on future shipping emissions (Scenario 3 - S3) and b) the increased use of methane and methanol as alternative fuels in 2050 (Scenario 8 - S8).

Ensemble model results were combined with population data for calculating population-weighted concentrations of legislated atmospheric pollutants for 30 Mediterranean coastal cities, representing exposure of city inhabitants to current and predicted future air pollution levels.

The findings of the present study reveal significant annual city average reductions of SO_2 and $PM_{2.5}$ shipping related exposure for both S3 (89.78 % reduction) and S8 (96.22 % reduction), while shipping induced NO_2 city-average exposure levels were efficiently controlled in S3 (42.74 % reduction) but not in S8 (4.39 % reduction). The reported results need to be specifically considered in the development of policy recommendations on shipping emission control for the Mediterranean region.

* Corresponding author.
E-mail address: evfragkou@auth.gr (E. Fragkou).

https://doi.org/10.1016/j.atmosenv.2025.121347
Received 8 January 2025; Received in revised form 1 May 2025; Accepted 8 June 2025
Available online 23 June 2025

1. Introduction

Mediterranean coastal areas are susceptible to deterioration of air quality related to shipping emissions, due to the increasing number of vessels calling in Mediterranean ports within the last decade, dictating the need for introducing effective air pollution mitigation measures to reduce the related health and environmental impacts. According to the DNV Maritime Forecast to 2050 report, global maritime transport is expected to rise significantly until 2035 and then remain stable towards 2050 (DNV-GL, 2019). The Mediterranean Sea, strategically located at the crossroads of three major maritime passages, namely the Strait of Gibraltar, the Suez Canal, and the Bosporus Strait, is a traditional exchange hub largely affected by economic growth and intensification of international trade. As the Mediterranean basin represents an important transit lane for international shipping, shipping activity in the area is expected to expand in line with the global growth of seaborne trade.

The assessment of the impact of maritime transport emissions on air quality in European coastal areas has been examined with the use of monitoring data, receptor and dispersion air quality models in several studies, collected and reviewed by Viana et al. (2014, 2020). The majority of these studies examined the influence of shipping emissions on PM components and concentrations in specific locations and over limited historical time periods. The number of studies focusing on the Mediterranean region were underrepresented compared to studies covering other European regions, such as the Baltic and the North Sea. The review studies underline the importance of the shipping sector as a significant contributor of gaseous and particulate pollutants (NO_x, SO_2, PM, and VOC) in locations particularly in the vicinity of harbours of coastal Mediterranean urban areas.

Accurate and reliable assessment of shipping and port-sourced air pollution requires monitoring data of high quality and coverage, hindered by a lack of appropriate on- and offshore air pollution measurement stations (Mueller et al., 2023) . Air quality dispersion models are the scientifically relevant tools recommended for air pollution assessment studies by EU legislation, as they provide information on spatial and temporal variation of pollutant concentrations. The impact of shipping emissions on air quality in the Mediterranean area has been assessed with the use of dispersion models either based on the application of an individual model or via model intercomparison studies, focusing on selected Mediterranean areas or cities.

The review study by Toscano (2023) provides quantified evidence from receptor and dispersion models on the contribution of shipping emissions to air pollution levels of 30 European ports of the Mediterranean region, between 2002 and 2018. The findings suggest higher SO_2 shipping contribution in port areas, while shipping related NO_2 levels account for a higher percentage of total NO_2 concentrations in the urban center. The study reports average SO_2 and NO_2 contributions of 46 % and 30.65 % respectively in air quality levels of port areas in examined cities, supporting the IMO decision for designation of the Mediterranean Sea as a Sulfur Emission Control Area (SECA) from January 2025 and the necessity for a Mediterranean Nitrogen Emission Control Area (NECA). The study by Durán-Grados et al. (2022) quantified the effect of maritime transport emissions in the air quality of the Strait of Gibraltar (Spain) and the coastal cities in the area, by using the CALPUFF dispersion model for 2017. The calculated annual average values of SO_x and NO_2 revealed that the contribution of maritime traffic to air quality levels can reach up to 20–25 % for the most susceptible locations, such as in the area of Algeciras. The study by Fink et al. (2023) presents the results from the model intercomparison exercise on quantifying NO_x and O_3 shipping contribution in the Mediterranean region, performed in the SCIPPER project. All five regional chemistry transport models participating in the study calculated a high shipping contribution on total NO_2 levels, particularly on the main shipping routes and in coastal regions (ranging from 25 % up to 85 % locally). The issue of inter-model variability is emphasized in the study and the findings recommend the use of ensemble modelling to address the uncertainties and limitations of individual models. None of the reported modelling studies examined the potential future impact of ships on the Mediterranean regional scale under different emissions scenarios, which is the focus of the present study.

The health impacts attributed to shipping emissions have been investigated in several studies, and the most representative research papers have been reviewed and analyzed by Mueller et al. (Mueller et al., 2023). The review findings confirm the causal link between shipping emissions and mortality/morbidity incidences, reporting around 265,000 premature deaths globally attributable to shipping related atmospheric pollution. Only two out of the 32 studies reviewed in total focused on the Mediterranean Sea area, highlighting the research gap in assessing the health burden due to atmospheric pollutant concentrations caused by shipping emissions over the area. Viana et al. (2020) showed that the significant contribution of shipping emissions in $PM_{2.5}$ levels in coastal cities (9,25 % annual average based on receptor modelling results in 8 Mediterranean coastal cities) increases total-cause mortality, cardiovascular and respiratory hospital admissions.

In response to the environmental and health issues associated with high SO_2 emissions from ships, the IMO has established Sulfur Emission Control Areas (SECAs) in susceptible areas, where the limit of sulfur content in the fuel is 0.1 % since January 1, 2015. There are currently five SECAs, covering North America, the US Caribbean Sea Areas, the North and Baltic Seas and the recently designated (since May 1, 2025) Mediterranean Sea. In areas outside SECAs, the IMO implemented regulations on shipping emissions, where the sulfur content of the ship fuel is required to be reduced to 0.5 % from 3.5 % as of January 2020, while the EU Directive 2005/33/EC requires all ships at berth or anchorage in European harbours to use fuels with a sulfur content of less than 0.1 % by weight from January 1, 2010, compared to the previous limit of 4.5 %. These measures have proven to be effective based on the data of relevant studies. Schembari et al. (2012) reported results of AQ measurements performed on board of a cruise ship at different Mediterranean harbours in selected days in 2009 and 2010, to cover a period before and after the regulation entered into force. The results suggested significant air quality benefits in the majority of the examined harbours, showing an average decrease of the daily mean SO_2 concentrations by 66 %.

Model simulations using future emission scenarios allow for quantified evaluation of the efficiency of pollution reduction strategies, such as the IMO regulations. In this frame, modelling results are particularly useful for regulators in policy development and air quality management. The Ship Traffic Emission Assessment Model (STEAM) model was applied to support the analysis of air quality measurements obtained from the coastal Atmospheric and Marine Research station at the Finnish Utö Island to identify trends in SO_2 concentrations in response to the SECA designation in the Baltic Sea (Maragkidou et al., 2024). The long-term analysis of high time resolution air quality data, covering a 15-year period (2006–2020) from a station in the vicinity of a heavily trafficked ship lane, revealed a significant reduction of measured SO_2 three-year averaged concentrations, with each averaging period corresponding to a further tightening of sulfur content limit in marine fuels. The study provides scientific evidence in support of emissions regulations targeting the shipping sector for improving coastal air quality.

Shipping emissions can be transferred further inland of coastal cities and contribute to urban coastal population exposure to increased air pollutant levels, resulting in detrimental health effects. Jang et al. (2023) estimated the share of maritime transport emissions in the $PM_{2.5}$ concentrations of the coastal city of Busan using a receptor and a dispersion model and calculated the difference before and after the implementation of emission reduction regulations. PMF receptor model results showed a significant decrease in shipping related $PM_{2.5}$ components, following the 2020 regulation on cleaner marine fuels. $PM_{2.5}$ reduction was evident both in the port area (by 88.9 %) and further extending in the urban area covered by the study (by 81.3 %). The atmospheric dispersion model results were in agreement with the receptor model in that shipping emissions regulations in port regions can reduce total $PM_{2.5}$ levels further inland, particularly in the summer season. The scenario applied in the study by Viana et al. (2020) considered reduction in sulfur content of marine fuels due to the stringent standards imposed by MARPOL Annex VI in 2020 and demonstrated an average decrease in the number of $PM_{2.5}$-attributable premature deaths by 15% .

Considering the aforementioned research and knowledge gaps, the present study aims to:

- o estimate shipping contribution on air pollution levels at a Mediterranean scale, particularly focusing on the Mediterranean coastal area, using detailed and updated emissions data input from the STEAM model developed and applied in the EMERGE project, by means of a bottom-up approach and load-dependent emission factors.
- o assess the efficiency of two different strategies for reducing shipping related air pollution in the Mediterranean and selected coastal cities, taking into account both technological solutions (scrubbers, SCR) and recent policy decisions (SECA/NECA, alternative fuels).
- o demonstrate the results of an ensemble modelling approach based on the output of three widely used and evaluated regional or global scale atmospheric models.
- o employ the ensemble model results for calculating an exposure indicator for 30 selected Mediterranean coastal cities, which are expected to be useful policy-relevant information.

The ensemble methodology for assessment of the impact of shipping emissions on Mediterranean air quality targets the need for tackling the issue of comparability between modelling studies and regions in a consistent way across Europe and addresses the uncertainty inherent to individual models underlined by review studies. The methodology was developed and tested in the frame of the EMERGE project, which examined the effects of potential emission reduction solutions for shipping in Europe and specifically focused on the efficiency and implications of scrubber use for mitigating shipping related impacts on the atmospheric and the marine environment.

2. Methodology

The geographical borders of the Mediterranean domain defined for the calculations and the locations of the selected cities are shown in Fig. 1. Regional model results were regridded and standardized on a rectangular latitude-longitude grid with a 0.05 × 0.05° resolution and extents defined as [30N … 47N, 8W … 38E].

The DPSIR (Drivers-Pressures-State-Impact-Response) methodological framework has been used as an integrated approach to quantify the contribution of shipping to air pollution under 2018 baseline conditions and under two future emission abatement scenarios for 2050, both considering high increase in ship traffic. To assess the air pollutant concentrations caused by shipping emissions, the ensemble annual and seasonal means of CMAQ, SILAM and EMEP model calculations were employed.

For both the 2018 baseline simulation and the two future selected scenarios , two simulations were performed to examine the contributions of shipping. The STEAM model's shipping emissions were incorporated in the total emissions inventory used for the first simulation, which is referred to as the base run. The shipping emissions were excluded from the second simulation. Subtracting the concentrations in the second simulation from the first one yielded the contributions from shipping.

2.1. Emissions calculation

Ship emission simulations have been performed using the Ship Traffic Emission Assessment Model (STEAM) (Jalkanen et al. 2009, 2012, 2021; Johansson et al., 2017). Ship emission inventories are produced for the baseline year 2018 and two different future scenarios in 2050. The ship emission dataset covers the European region (Domain: [30N … 72N, −30E … 60E]) on a latitude-longitude spatial resolution of 0.05° × 0.1° and a temporal resolution of 1 h. Emission data is produced for two height layers: 0–36 m height and 36–1000 m height based on the stack height of each ship.

STEAM model uses automatic identification system (AIS) data to describe the spatial and temporal variation of shipping traffic. Also, a

Fig. 1. The Mediterranean region domain used in regional simulations.

technical description of each modelled vessel is included. AIS data used in this study is from Orbcomm Ltd. and includes both terrestrial and satellite position reports. The ship's technical database is obtained from S&P Global. In the EMERGE project, the STEAM model was refined to simulate the effects of wind, sea waves, sea currents, and sea ice on ship's fuel consumption and emissions. Data on scrubbers (Exhaust Gas Cleaning Systems -EGCS) installations on ships was collected from IMO GISIS (Global Information System for International Shipping) system. The emission reduction performance of the most utilized abatement technologies (such as wet scrubbers, SCR, DOC and DPF) and emission factors for metals and PAHs in the STEAM model were updated within the EMERGE project based on existing literature data and the results of EMERGE measurement campaigns (Grigoriadis et al., 2024).

2.1.1. Baseline year shipping emissions

Year 2018 was selected as the baseline year for analyzing the changes in shipping emissions, representing the baseline situation during the EMERGE project, as the most recent year when information on shipping traffic and inventories for land-based emission sources to air (CAMS-REG-v4.2 inventory) were available. This year was considered to be sufficiently recent, and this selection avoids possibly exceptional effects caused by the more recent COVID-19 pandemic.

The emission inventory for the baseline year was produced using the STEAM model. Effects of wind, sea waves and sea currents have been included in the modelling using data from Copernicus climate data store (CDS) and Copernicus marine services (CMEMS). The effect of sea ice is also included in the modelling although this is not relevant for the Mediterranean Sea. All weather and sea state data fields are updated on a temporal resolution of 3 h. In the baseline year 2018, 30000 vessels were identified in the Mediterranean Sea, while 20000 of these were transmitting an IMO registry number. The number of vessels equipped with scrubbers in the Mediterranean Sea has increased from approximately 50 scrubber ships in 2014 to over 2500 scrubber ships in 2022. The majority (>80 % in 2022) of these scrubbers are open-loop type.

2.1.2. Future scenarios of the shipping emissions

A total of eight ship emission scenarios were developed within the EMERGE project to account for future trends in the maritime transport sector as a total environmental pressure to the atmospheric and marine environment and respective emissions inventories were produced for 2050 using the STEAM model. An overview of the assumptions behind all the scenarios is shown in the Appendix (Table A.1). Shipping traffic in 2050 is based on the scaling of AIS data from the respective values in the baseline year 2018. This implies that the spatial distribution of the shipping routes and their relative traffic flows were assumed to be the same in 2018 and 2050.

For the purposes of scaling the AIS data from 2018 to 2050, the EMERGE project considered two different projections of the future transport volumes following the suggestions by DNV-GL (2020), including also the changes of ships in terms of efficiency and ship size. The two projections, the low-growth projection and the high-growth projection, were chosen to study differences between two extreme situations and to understand the range of potential impacts. Scenarios S3 and S8 both follow the high-growth scenarios defined by DNV-GL (2020), which is similar to the scenario 16 from the Third IMO GHG Study (Smith et al., 2015). This transport projection is based on the representative concentration pathways (RCP) 2.6 and the ship transport work is assumed to increase by 180 % from 2018 to 2050. Changes in the transport work by shipping in the Mediterranean Sea in 2018 and 2050 are shown in the Appendix (Table A.2). The scenarios also accounted for the use of abatement equipment, such as scrubbers and Selective Catalytic Reduction (SCR), and the use of alternative fuels (Table A.3). The use of scrubbers was modelled using an economic model, i.e. ship owners were assumed to use scrubbers when it was profitable, in combination with potential restrictions on the use of scrubbers. Scrubber installation in vessels has recently increased as a popular abatement solution due to the relatively low retrofitting cost and the efficiency in removing SO_x and PM_x from engines' exhaust gases by spraying sea water (open-loop system) or freshwater (closed-loop system) on them. In the scenarios for the future, sea and weather data were not used; instead a constant loss of the energy used due to weather equal to 8 % was applied for all ship traffic.

In this study, two contrasting situations were selected for atmospheric and water modelling simulations, with particular emphasis on the use of scrubbers. Scenario 3 (designated here as S3) and Scenario 8 (S8). S3 is a high-pressure scenario, where there are no further measures taken to reduce the use of fossil fuels in shipping. Sulfur and nitrogen oxide emission control areas (SECAs and NECAs) were assumed to be introduced in all European sea regions within 200 nautical miles from the coastline, along with a significant use of open-loop scrubbers and SCR systems. A 200 US$ fuel price difference between HFO and VLSFO was presumed in S3, resulting to an adoption rate of scrubbers varying between 4 % for general cargo ships to 74 % for container ships. In Scenario 8 (S8), the shipping sector was assumed to rely on a substantial use of Liquified Natural Gas (LNG) and methanol as alternative fuels, aligned with the IMO initial strategy to reduce GHG emissions by 50 % by 2050 compared to 2008. S8 assumes no use of scrubbers and SCRs.

2.1.3. Land emissions 2018 and 2050 ECLIPSE MFR land emissions

CAMS emissions (Kuenen et al., 2022) for the land-based sectors were prepared to be used as an input to the air quality models for the baseline year 2018. The CAMS regional emissions inventory is a widely used emissions dataset for air quality model simulations, providing emissions data for 13 sectors, including shipping. Within EMERGE, the CAMS shipping emissions were replaced with those calculated by STEAM. The land emissions for year 2050 are based on emissions compiled in the SCIPPER project scaling CAMS emissions for year 2015 with year 2050/2015 factors derived from ECLIPSE v6b MFR (Maximum Feasible Reduction) global emission scenarios (Höglund-Isaksson et al., 2020; Klimont et al., 2017). NO_x total sector 2050 emissions (excluding shipping) demonstrate the highest reduction among pollutants compared to the 2018 levels, accounting for 65 %, followed by a 34 % reduction of total $PM_{2.5}$ emissions and a 21 % reduction in the case of SO_x emissions.

2.2. Dispersion models - set up

For the ensemble analysis, the results of the regional scale models EMEP and CMAQ and the global-regional SILAM model were used.

The EMEP MSC-W model (version rv4.45 used) is a limited-area, terrain following hybrid coordinate model calculating air concentrations and deposition fields for major acidifying and eutrophying pollutants, photo-oxidants and particulate matter (Simpson et al., 2012, 2020). It has been developed at the Meteorological Synthesizing Centre-West (MSC-W) of the European Monitoring and Evaluation Programme (EMEP) at the Norwegian Meteorological Institute to perform model calculations in support of the Convention on Long Range Transboundary Air Pollution (CLRTAP) and is one of the key tools within European air pollution policy assessments. The chemical mechanism of the model EmChem, version 19a (Simpson et al., 2020), builds on surrogate VOC species and has 171 gas-phase and heterogeneous reactions. The aerosol classes used in EMEP include fine-mode nitrate and ammonium, other fine-mode particles, e.g., sulphate, elemental carbon (EC) and organic aerosol, coarse nitrate, coarse sea-salt and coarse dust. The model assumes equilibrium between the gas and aerosol phase, using the MARS equilibrium module (Model for an Aerosol Reacting System) of Binkowski and Shankar (1995).

SILAM (version 5.8) is a global and regional scale chemical transport model. A new version of the model, which evaluates tropospheric chemistry using the Carbon Bond Model, version 05 (CBM05) (Yarwood et al., 2005), was developed and applied within the frame of EMERGE. This scheme includes a new solution to the common problem of all carbon-bond schemes; i.e., that they all are not positive semi-definite. All the major air pollutants (e.g., ozone, NO_x, CO) included in the CBM05 model are included in the output of SILAM runs. Additionally, the model considers sea salt, dust, and secondary organic aerosols, and two heavy metals: lead (Pb) and cadmium (Cd). The current setup of the model is based on CAMS regional setup, which uses CAMS regional emissions inventory (version 4.2) to estimate anthropogenic emissions, complemented with shipping emissions by STEAM. For regional (European) scale simulations, at $0.05 \times 0.05^\circ$ resolution, SILAM was driven by ECMWF operational meteorology. SILAM is optimized and operationally run with ECMWF meteorology and typically reaches highest correlation and smallest bias with this meteorology, while the bias e.g. for ozone is often larger with WRF-meteorology. The only downsize for using ECMWF meteorology is the slightly lower resolution that might lower the model performance compared with the higher resolution WRF-meteo. This might be important e.g. near the coastal lines or in hilly/mountainous regions, but only if the model resolution allows to resolve these fine structures.

The Community Multiscale Air Quality (CMAQ) model, developed by the U.S. Environmental Protection Agency, is a widely used open-source system for simulating atmospheric processes. This study utilized CMAQ version 5.3.2 (US EPA, 2020), which employs a “1-atm” approach to account for pollutant interactions across regional and urban scales, incorporating the Carbon Bond version 6 chemical mechanism (Luecken et al., 2019). Key components of CMAQ include the Meteorology-Chemistry Interface Processor (MCIP) (Otte and Pleim, 2010), the Initial Condition processor (ICON), the Boundary Condition processor (BCON), and the Chemistry Transport Model (CTM) (Otte and Pleim, 2010). To establish initial boundary conditions for the CMAQ model, output from the hemispheric CMAQ simulations conducted by the United States Environmental Protection Agency (US EPA) for the northern hemisphere (US EPA, 2021) was used. SMOKE version 4.6 ((The institute for the Environment - The University of North Carolina at Chapel Hill, 2018) was used to process anthropogenic emissions. The Model of Emissions of Gases and Aerosols from Nature (MEGAN, version 2.0.4; Guenther, 2024) was used to produce biogenic emissions for CMAQ model.

Meteorological input fields for CMAQ and EMEP simulations were prepared using the Weather Research and Forecasting (WRF) model version 4.2.1 (Skamarock et al., 2019). The performance of the WRF model, configured with a 15 km spatial resolution for 2018, was evaluated for meteorological representation across stations within the modelling domain. Model outputs were compared against observed meteorological data from 712 stations in the Mediterranean region. Observational data for relative humidity (RH), wind speed (WS) and 2-m (near surface) air temperature (T2) were obtained from the global hourly integrated surface data observations, from National Oceanic and Atmospheric Administration (NOAA) (available from: https://www.ncei.noaa.gov/data/global-hourly/access/).

The evaluation demonstrated strong agreement between modelled and observed values. For the daily averaged T2, the mean coefficient of determination (R^2) across 712 stations was 0.965, with a mean bias of -0.73 °C, root mean square error (RMSE) of 2.22 °C, and an index of agreement (IOA) of 0.967. Fig. 2 presents the spatial distribution of daily-averaged RMSE values for T2 across the Mediterranean region in 2018. RMSE values ranged from 0.72 °C to 14.35 °C, with the majority of stations showing errors below 3 °C. Furthermore, the model's performance for RH yielded a mean R^2 of 0.588, a bias of -1.30 %, and an IOA of 0.812. For WS, the mean R^2 was 0.502, with a bias of 0.87 m s^{-1} and an IOA of 0.673.

The set-up specifications of the models in relation to their employment in the current study are summarized in the following table Table 1.

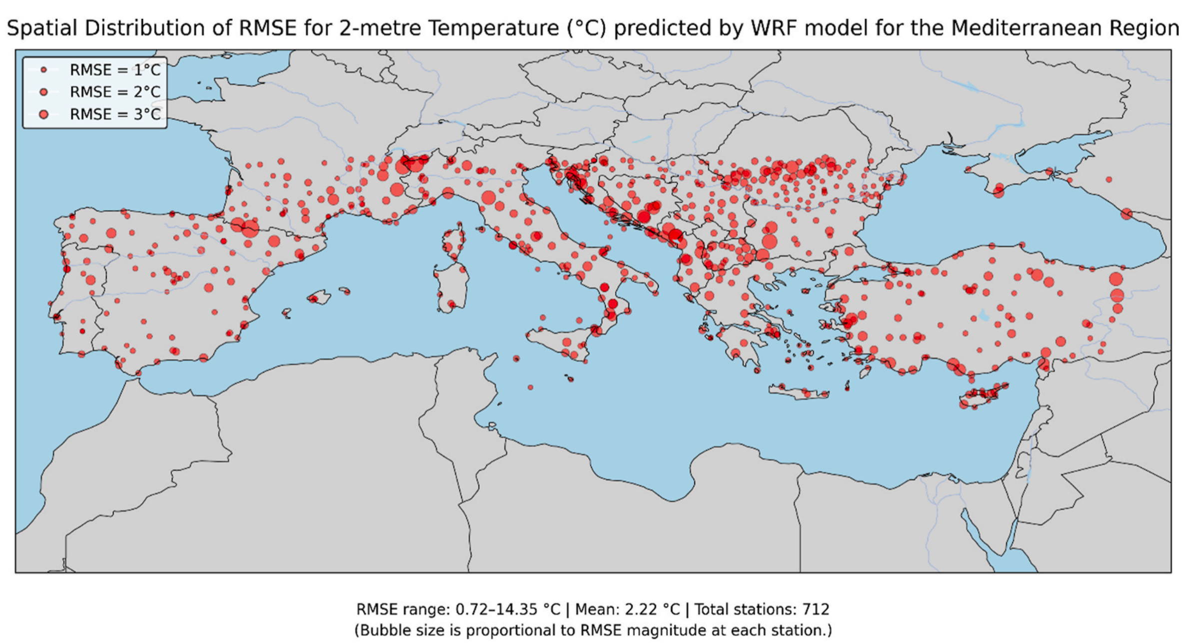

Fig. 2. Spatial distribution of RMSE (°C) for daily averaged T2 predicted by WRF model across the Mediterranean region for 2018. Each red bubble represents a monitoring station, with bubble size proportional to the RMSE magnitude. RMSE values ranged from 0.72 °C to 14.35 °C, with a mean of 2.22 °C across 712 stations. (For interpretation of the references to colour in this figure legend, the reader is referred to the Web version of this article.)

Table 1
Dispersion model set-up.

Model	Grid resolution	Boundary conditions	Meteorological driver	Chemical mechanism
CMAQ v5.3.2	15 × 15 km	NCEP/FNL	WRF v4.2.1	Carbon Bond 6 for gas-phase chemistry, Aerosol Module 6 for aerosol processes
EMEP v. rv4.45	15 × 15 km	Provided with the open-source model distribution	WRF v4.2.1	EmChem, version 19a
SILAM v 5.8	5 × 5 km	IFS-boundary	ECMWF operational	Carbon Bond 05 with SOA formation

2.3. Ensemble modelling

The methodology for producing ensemble concentration maps obtained from a fusion of the three dispersion models, SILAM, EMEP and CMAQ is based on established ensemble modelling approaches (Vautard et al., 2009). For the purposes of the present study, only annual ensemble averages of absolute contributions and shipping contributions were calculated and the ensemble mean was used instead of the ensemble median.

A further complication is that the constituent models' output grids use different horizontal resolutions (15 km for EMEP and CMAQ, 5 km for SILAM) and native geographical projections. For this reason, both EMEP and CMAQ concentration fields were re-projected and interpolated to match the SILAM latitude-longitude output grid, before calculating the ensemble mean. Bilinear interpolation was used, in order to avoid spurious overfitting and the potential appearance of negative concentration artifacts that could occur with higher-order interpolation. For output grid cells where one or two model values were unavailable, the mean of the remaining two or the single remaining model was used.

$$\text{Population weighted concentration}\left(\frac{\mu g}{m^3}\right) = \frac{\Sigma(\text{model predicted concentration per grid of city})*(\text{population per grid of city})}{\text{total population in the city}} \quad \text{Equation 1}$$

2.4. Population weighted concentrations

The initial phase of the population-weighted concentration analysis included the definition and application of criteria for the city selection process. The two factors considered included population density and proximity to heavily trafficked shipping routes in the Mediterranean region. In this frame, a list was drafted including cities along the Mediterranean coast with populations exceeding 300,000 residents. Venice was selected as an exception because it is one of the case study regions in the EMERGE project, despite having a population slightly below the specified threshold. The 30 cities chosen for this study are visually represented in Fig. 3. To maintain consistency in the results across all modelling groups during data collection, predetermined latitude and longitude boundaries were established for each city. Additionally, each city's boundary extended approximately 25 km from the coast.

The predefined latitude and longitude limits for a given city were used to extract grid and population data from the 1 km resolution gridded population file of the European Joint Research Centre (JRC-GEOSTAT 2018), reporting the number of residents for the year 2018 per 1 km^2 in Europe. In cases where JRC population data was unavailable for Mediterranean cities outside the European domain, WorldPop population data was employed. To ensure consistency, concentrations for each pollutant were re-gridded to match the grid generated for the population data. Equation (1) outlines the calculation of population-weighted concentrations for each city. The model-predicted concentrations per grid were multiplied by the population in the corresponding grid cell. The sum of these multiplications was then divided by the total population in the city, resulting in population-weighted concentrations reported by each modelling group in units of μg/m^3.

The average model results (ensemble model means) produced following the methodology outlined in section 2.3 were employed for calculating population-weighted concentrations, as a policy-related indicator of health impact on the population of the examined cities.

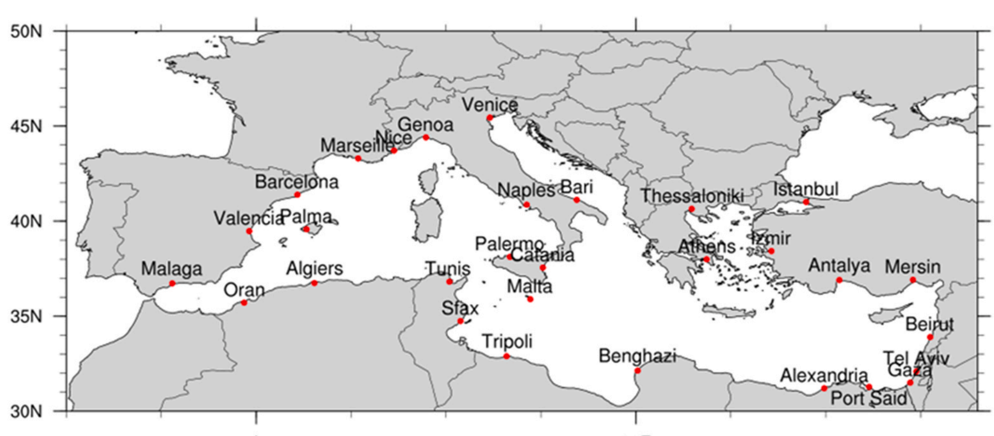

Fig. 3. Map of the 30 Mediterranean cities selected for population-weighted concentrations analysis.

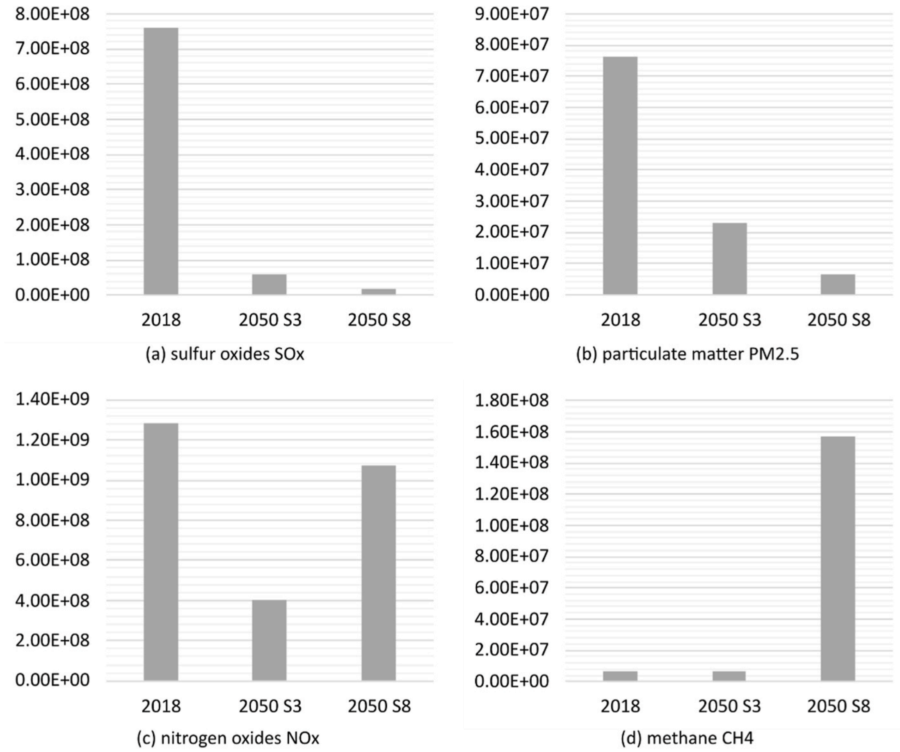

Fig. 4. STEAM calculated annual emissions (in kg) of sulfur oxides, particulate matter, nitrogen oxides and methane from shipping in the Mediterranean Sea in 2018 and in two scenarios (S3 and S8) in 2050.

3. Results and discussion

3.1. Estimation of shipping emissions

Fig. 4 shows the total annual emissions of particulate matter ($PM_{2.5}$), methane (CH_4), nitrogen oxides (NO_x), and sulfur oxides (SO_x) from shipping in the two scenarios in 2050. The calculated emissions for all pollutants are shown in the Appendix (Table A.4). A significant reduction of SO_x and $PM_{2.5}$ shipping emissions is achieved by implementing both S3 and S8. SO_x emissions are reduced by ~93 % in the case of S3 implementation with high scrubber use, and by ~97 % in S8 with the introduction of sulfur-free alternative fuels. The results agree with literature reported reductions of SO_x emissions by 98 % with the use of scrubbers (Kristensen, 2012). $PM_{2.5}$ emissions show a similar trend with reductions of ~73 % for S3 and ~90 % for S8. Methane shipping emissions remain unchanged between the baseline scenario and implementation of S3, while the use of methanol and methane as alternative fuels in S8 results in their increase by a factor of 16. The use of SCR in the designated NECA Mediterranean region, as depicted in S3, efficiently reduced NO_x shipping emissions by ~69 %. High efficiency of SCR systems in reducing engine-out NO_x emissions from ships is reported in the literature, with more pronounced reductions achieved in the case of higher exhaust temperatures (Aakko-Saksa et al., 2023). NO_x amounts emitted from ships in the Mediterranean region are reduced by 13 % when the use of alternative fuels methane/methanol is enhanced (S8).

3.2. Ensemble model results

Ensemble model results regarding the spatial distribution of total NO_2 concentrations for the baseline year 2018 are dominated by land-based contributions with localized maxima in the Po valley region as well as around the major European and African conurbations with a spatial maximum of around 33 μg/m^3 near Cairo (Fig. 5). The largest shipping contribution to NO_2 appears around shipping routes in the Gibraltar and Marmaras straits (up to 18 μg/m^3) amounting to about 95 % and 80 % of total concentrations for the two corresponding areas, while lesser local minima appear around major port areas. In land areas up to a few km off the Mediterranean coast, the relative shipping impact ranges between 20 and 45 %, with isolated peaks of about 50 % near the port hot-spots. These results are in line with previous ensemble model estimates by Fink et al. (2023) of a shipping contribution of 25 %–45 % to total NO_2 levels. Merico et al. (Merico et al., 2017) found similar results in a study examining four port cities in the Adriatic–Ionian Sea, with shipping impact of up to 32.5 % on total NO_2. Under S3 for 2050 (Fig. 6), the shipping contribution to total NO_2 levels is reduced by more than 50 % along the main shipping routes, in comparison to baseline. The spatial maximum contributions in the Gibraltar and Marmaras strait persist, although they are reduced by about 40 % compared to baseline. Similarly to the calculations of emissions reductions (Fig. 4), S8 (Fig. 7) induces a much smaller reduction of NO_2 concentrations along offshore routes compared to S3, in the order of 10 %, while spatial maxima are reduced by 15 %.

The baseline 2018 shipping contribution to O_3 concentrations indicates a mixture of VOC-limited and NO_x limited regimes in different regions. The contributions appear positive, up to 7.7 μg/m^3 (amounting to almost 9 % of total O_3) in a wide area around offshore shipping routes with the effect gradually diminishing near coastlines. On the other hand, shipping contribution appears strongly negative, up to −7.0 μg/m^3 (amounting to about −11 % reduction of total O_3) near Gibraltar, along the main Aegean shipping route as well as close to port areas, where NO_2 shipping contribution is higher due to O_3 titration by the primary emitted NO. Under S3 for 2050, the titration maximum in Gibraltar and along the Aegean routes is largely diminished, leaving a strong negative contribution just in the Marmaras strait (Fig. 6). However, the positive contribution to offshore routes is reduced by almost 50 % compared to the 2018 baseline. Under S8, the negative contribution is reduced by about 12 %, but the positive contribution near the shipping routes slightly increases compared to the baseline (Fig. 7). Looking at the seasonal variation, it is important to note that mixed-signed contributions appear during the cold season while shipping has a net positive

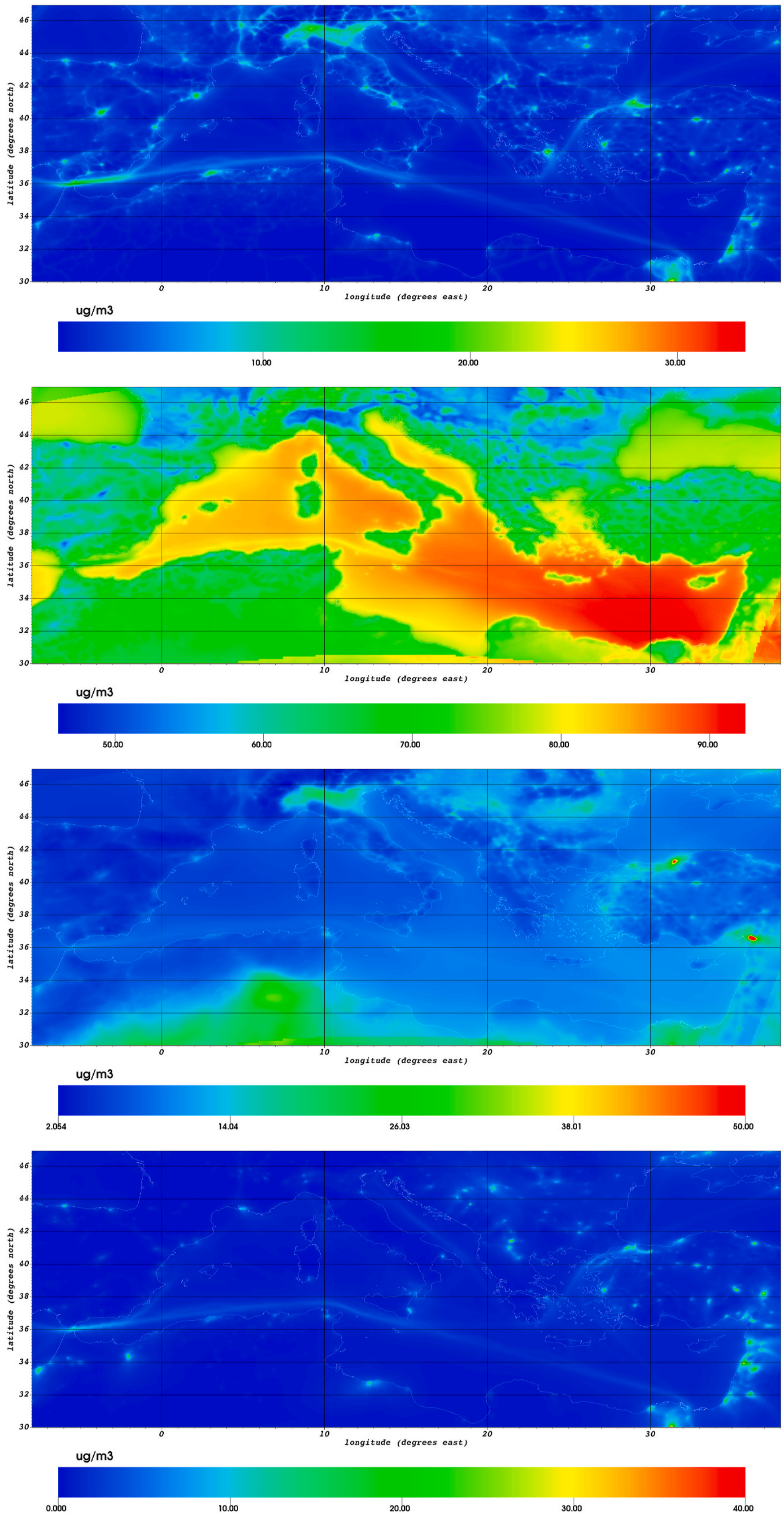

Fig. 5. Ensemble annual average pollutant (a. NO_2; b. Ozone; c. $PM_{2.5}$, d. SO_2) concentrations calculated for all emissions sources (including shipping from STEAM) for the 2018 baseline scenario.

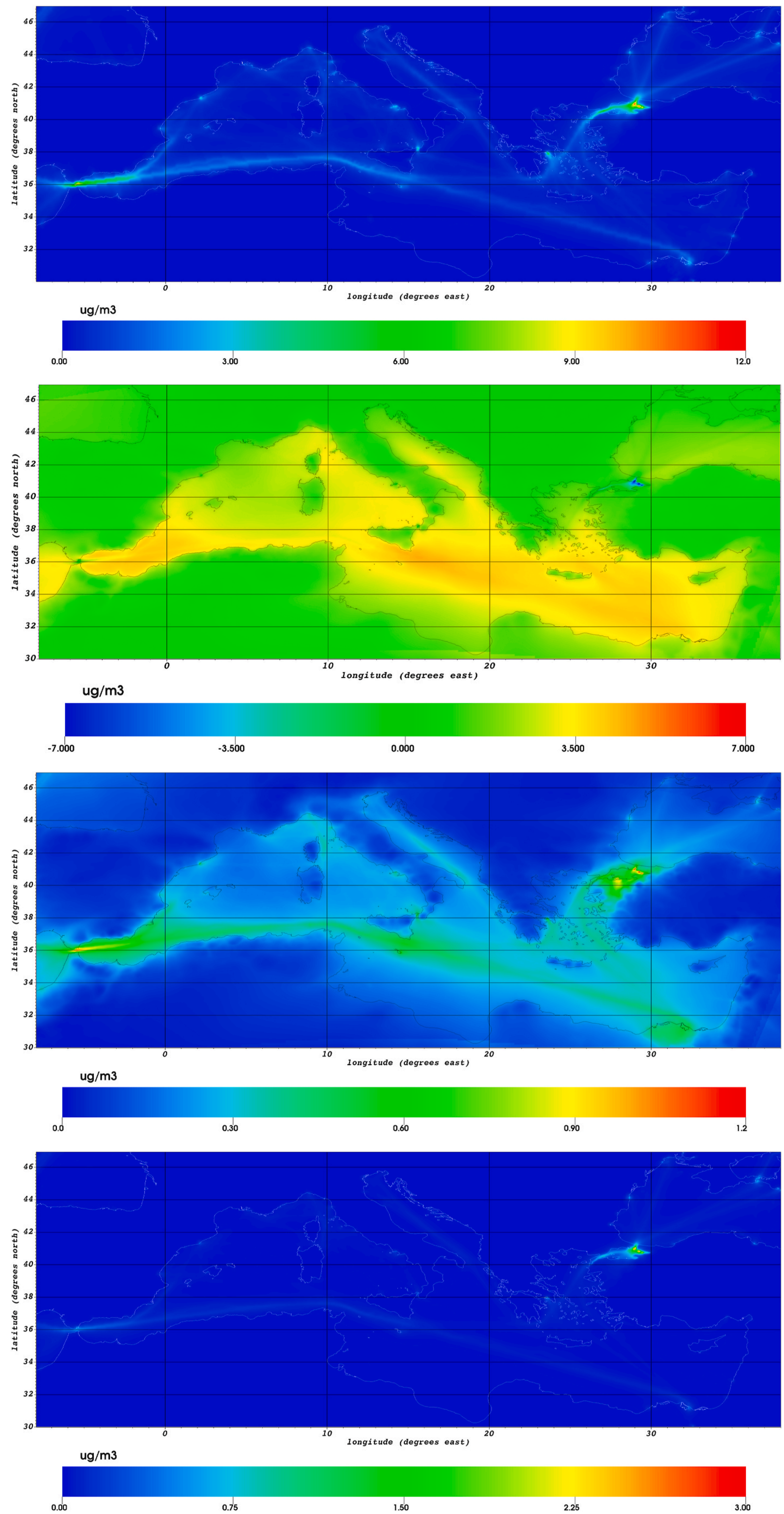

Fig. 6. Ensemble annual average shipping contribution pollutant (a. NO_2; b. Ozone; c. $PM_{2.5}$, d. SO_2) concentrations calculated for S3.

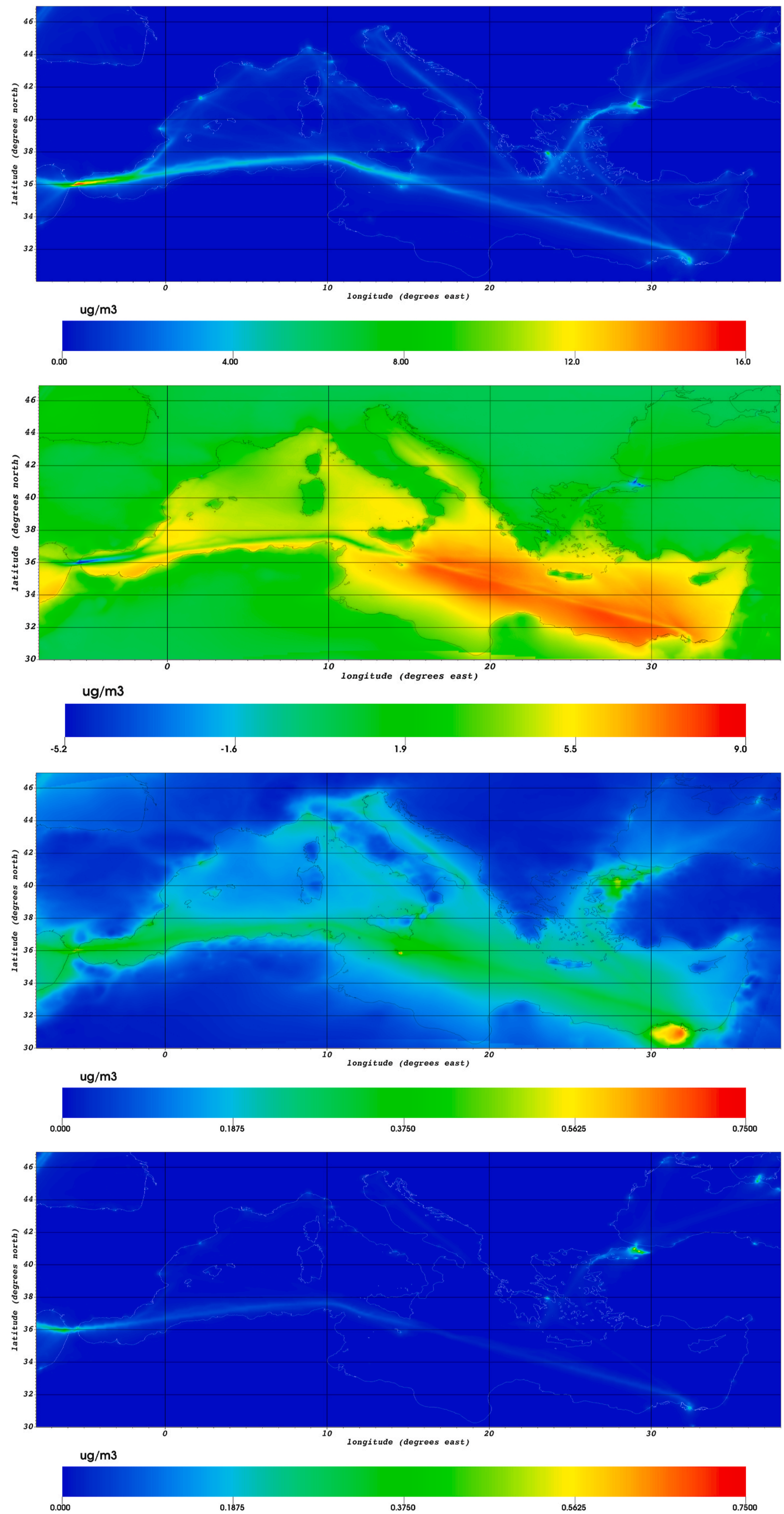

Fig. 7. Ensemble annual average shipping contribution pollutant (a. NO_2; b. Ozone; c. $PM_{2.5}$, d. SO_2) concentrations calculated for S8.

contribution during the hot season throughout the modelling domain.

Total baseline 2018 concentrations of $PM_{2.5}$ (Fig. 5) are dominated by contributions from Saharan dust, which appears stronger in SILAM by a factor of two, compared to the other two models, as well as in the Po Valley and the Nile delta areas and large point sources. The spatial maximum reaches 175 μg/m^3. The shipping contribution to $PM_{2.5}$ follows a similar spatial distribution to that of NO_2 with a spatial maximum of 5 μg/m^3, representing almost 50 % of total $PM_{2.5}$ in the western Mediterranean and near the Gibraltar strait. However, the absence of sharp localised maxima makes the corresponding shipping plume appear much more extended, amounting to a contribution between 0.8 and 1.4 μg/m^3 over extended areas, representing 10 %–15 % of total concentrations over a strip along the coastline, which extends a few km inland. S3 for 2050 induces an almost spatially uniform reduction of up to 85 % in the shipping contribution to $PM_{2.5}$, with lesser reductions in major African and Asian ports (Fig. 6). S8 causes further reductions of the shipping contribution by about 35 % percent throughout the region (Fig. 7).

Finally, total 2018 concentrations of SO_2 (Fig. 5) are dominated by contributions of land-based point sources, with several spatial hotspots ranging between 10 and 40 μg/m^3. Contributions of shipping lanes are still sharply distinguishable with spatial maxima of about 11 μg/m^3 in the Gibraltar strait and 8 μg/m^3 near Istanbul, representing contributions of 93 % and 55 %, respectively, to total SO_2 concentrations. Along the Mediterranean coast, shipping contributions amount from 40 % of total SO_2 off-coast down to about 25 % a few km inland. Introduction of restrictions under S3 for 2050 would almost eliminate SO_2 shipping contributions by more than 90 %, for most of the Mediterranean regions (Fig. 6). However, near the Marmara strait the reduction is much smaller, about 50 %. Introduction of fuel replacement under S8 would further reduce the SO_2 shipping contribution throughout the Mediterranean (Fig. 7) by a percentage of about 95 % compared to the 2018 baseline.

3.3. Population weighted exposure analysis

Exposure to shipping-related air pollution is assessed by calculating population-weighted concentrations of pollutants in 30 selected cities. This analysis enhances the understanding of both the overall pollution levels associated with baseline and future shipping emissions, as well as the number of people exposed to these pollutants in the examined Mediterranean cities.

As shown in Fig. 8, exposure to total NO_2 levels is highest in Athens reaching a value of 20 μg/m^3, followed by Barcelona (18.50 μg/m^3), Tel Aviv (14.12 μg/m^3), Izmir (13.74 μg/m^3) and Istanbul (13.73 μg/m^3). The lowest exposure levels are calculated for Sfax (1.75 μg/m^3), Bari (4.59 μg/m^3) and Antalya (4.99 μg/m^3). Shipping contribution to NO_2 exposure is estimated to be significant in coastal areas, accounting for a city average of 16 % in the baseline scenario. Istanbul presents the highest shipping-related NO_2 population exposure at 5.50 μg/m^3 and a high shipping contribution of 41 %, while the highest shipping contribution to NO_2 exposure is estimated in Port Said (57 %) with a calculated exposure level to shipping-related NO_2 of 4.07 μg/m^3. Piraeus city in Athens and Barcelona also demonstrate high exposures to shipping related NO_2 (3.86 μg/m^3 and 3.45 μg/m^3 respectively), corresponding to a shipping contribution to total NO_2 exposure of 19 % for both cities, revealing the significant share of the shipping sector to total NO_x emissions in the particular urban areas. In regard to the population-weighted all-sector NO_2 concentrations (Fig. 8), for most European ports a reduction of about between 20 % and 60 % is predicted for 2050 under the S3 scenario, and slightly less for the S8 scenario. On the other hand, most of the North African and Middle East ports NO_2 concentrations exhibit the opposite trend by increasing in 2050 for both scenarios. Particularly in Beirut and Benghazi a rise of around 60 % is calculated for both S3 and S8. This difference implies that the observed reduction in European ports is caused by an all-sector reduction in NO_2 emissions, mainly due to the implementation of legislative reductions in transport and industry.

Isolating the shipping contributions to NO_2, it is evident that the implementation of a Mediterranean NECA in S3 for 2050 would cause a city-average significant reduction of around 43 % in weighted concentrations, becoming more pronounced in port cities with relatively low industrial density (Fig. 9). On the other hand, the S8 scenario fails to deliver any significant reduction of the shipping contribution for most of the cities.

In Fig. 10, the shipping contributions are plotted, isolating the winter (DJF) and summer (JJA) periods. For European ports, reductions under the S3 and S8 retain the same sign throughout the year, with the reduction effect varying across cities. For North African and Middle East ports however, reduction in S3 appears weaker during summertime while increases in S8 are also amplified.

Annual population exposure to SO_2 concentrations is at low levels, reaching a maximum value of 13 μg/m^3 in Izmir. Similar exposures are calculated in Beirut and Alexandria, while in the majority of the examined coastal cities the total average SO_2 exposure for the baseline year is around 2 μg/m^3. Shipping emissions have a higher contribution to total SO_2 exposure levels across cities, compared to NO_2, representing a city average value of 23 % for the baseline year. This contribution is

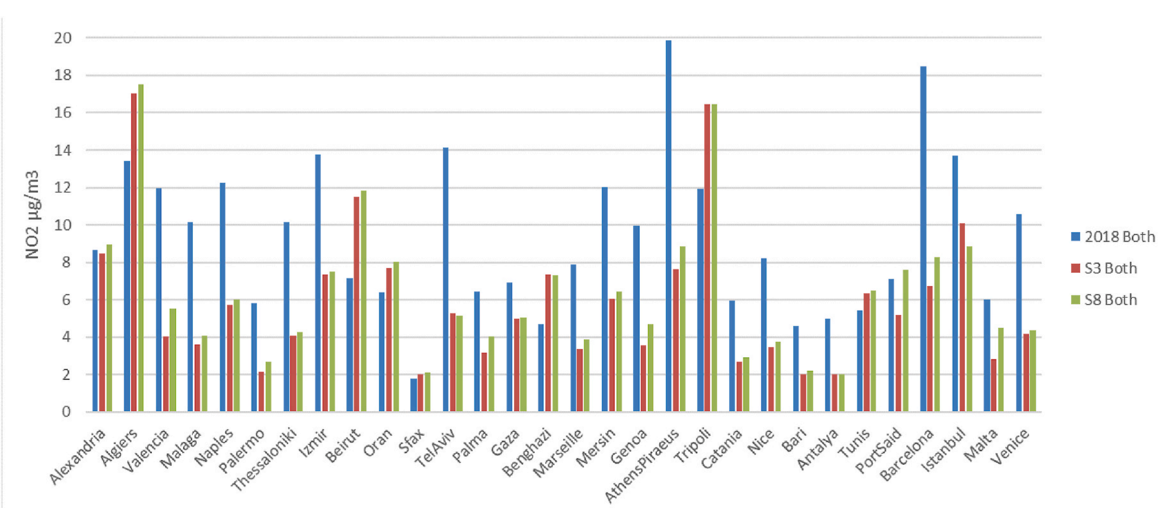

Fig. 8. Population weighted city exposures to total NO_2 ensemble annual concentrations for the baseline year and for S3 and S8.

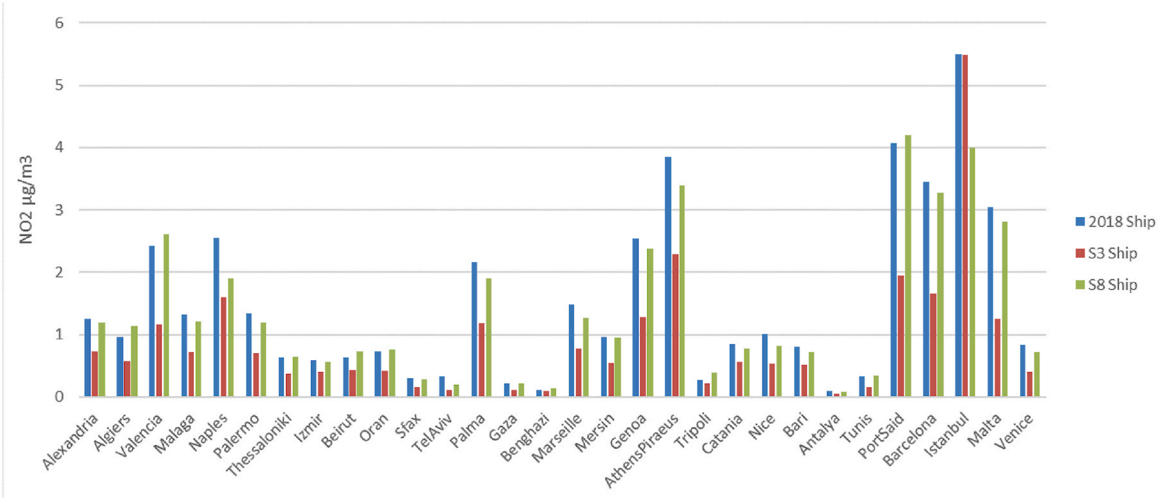

Fig. 9. Population weighted city exposures to shipping related NO_2 ensemble annual concentrations for the baseline year and for S3 and S8.

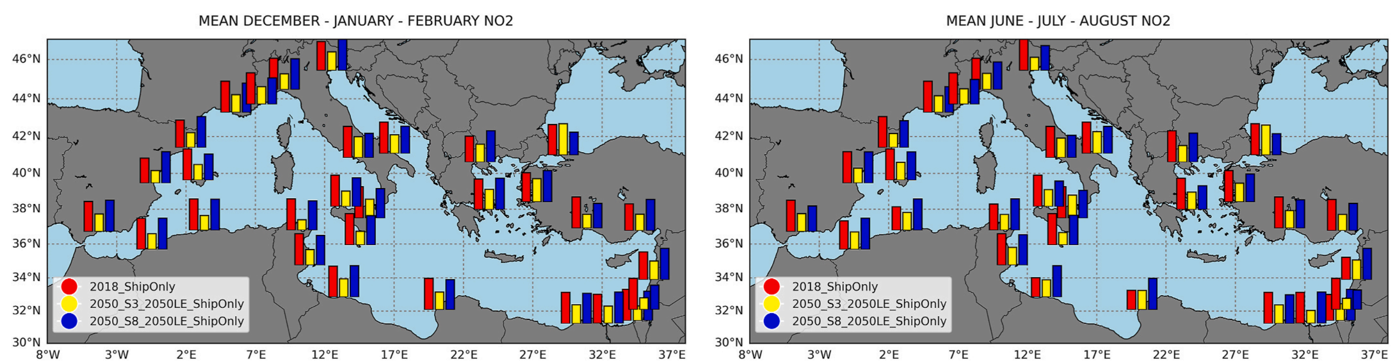

Fig. 10. Population weighted city exposures to shipping related NO_2 ensemble winter (left) and summer (right) concentrations for the baseline year and for S3 and S8.

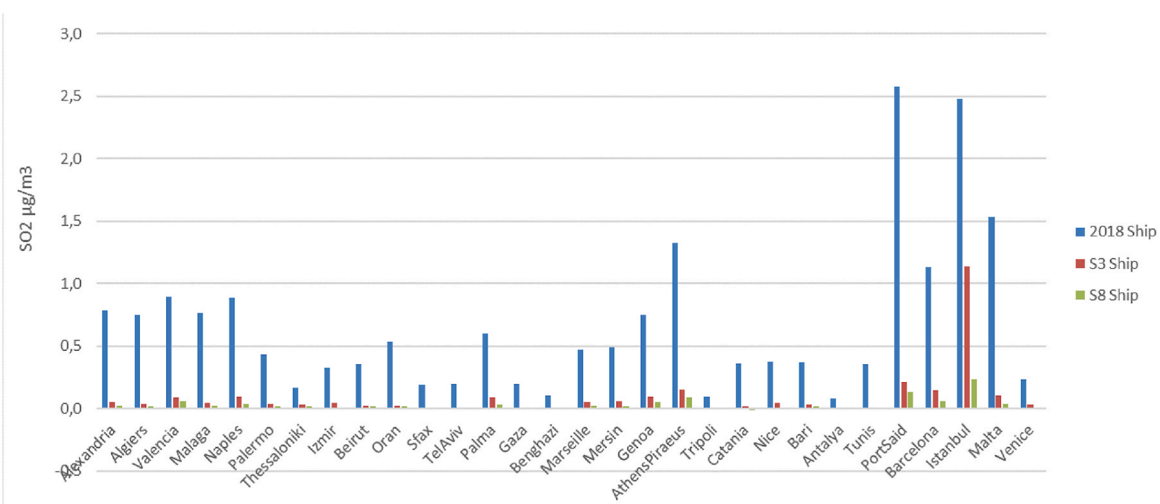

Fig. 11. Population weighted city exposures to shipping related SO_2 ensemble annual concentrations for the baseline year and for S3 and S8.

reduced to a city average value of 9 % for S3 and 4 % for S8. The cities exhibiting the highest shipping induced SO_2 weighted exposures are Port Said (2.58 μg/m^3), Istanbul (2.48 μg/m^3), Malta and Piraeus (Figure 11), as in the case of NO_2.

Considering the efficiency of the emission scenarios, SO_2 exhibits the largest relative reduction of all examined pollutants in 2050, both in terms of total weighted concentrations (between 62.79 % for S3 and 64.23 % for S8 as a city-average annual reduction) and shipping related exposure (between 89.78 % for S3 and 96.22 % for S8 as a city-average annual reduction). Of the two scenarios, S8 appears to be more effective in mitigating SO_2 contributions compared to S3.

Population-weighted exposures to $PM_{2.5}$ in 2018 are characterized

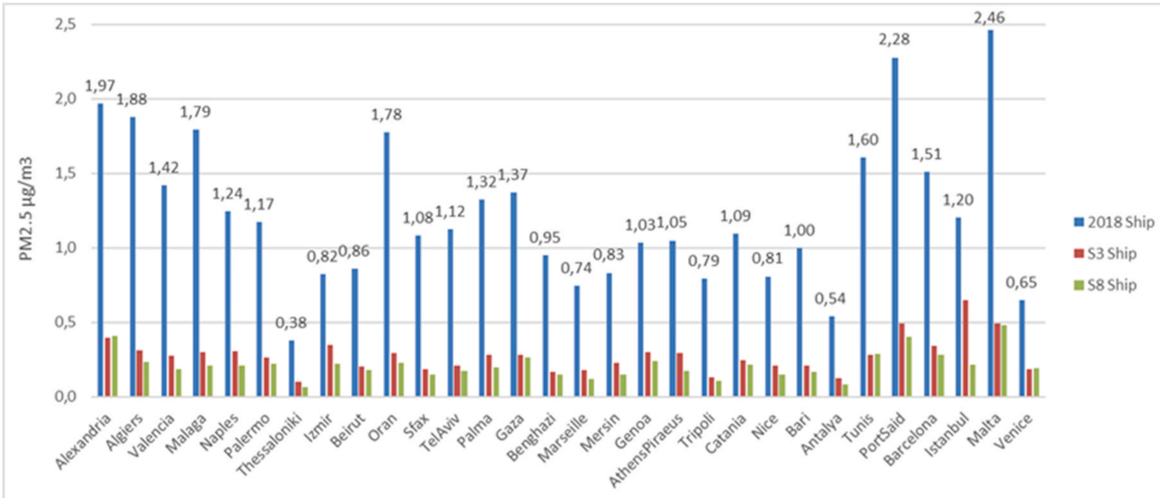

Fig. 12. Population weighted city exposures to shipping related $PM_{2.5}$ ensemble annual concentrations for the baseline year and for S3 and S8.

by high levels >10 $\mu g/m^3$ in 17 out of the 30 examined Mediterranean coastal cities, reaching up to 17.39 $\mu g/m^3$ in Istanbul. Across city average shipping contribution to $PM_{2.5}$ exposure accounts for 11 % in 2018, which is reduced to 5 % in S3 and further reduced to 4 % in S8. As shown in Figure 12, $PM_{2.5}$ exposure related to shipping emissions is on average 1.22 $\mu g/m^3$ across cities in 2018, with exposure values reaching up to 2.46 $\mu g/m^3$ in Malta, followed by Port Said (2.28 $\mu g/m^3$), Alexandria (1.97 $\mu g/m^3$) and Algiers (1.88 $\mu g/m^3$). Scenario efficiency in the case of $PM_{2.5}$ exposures follows a similar trend to SO_2, with reductions in total $PM_{2.5}$ exposure levels of 45.16 % for S3 and 46 % for S8, and higher reduction of shipping related exposures of 75.42 % and 81.13 % for S3 and S8 respectively. The reduction appears to be larger in ports with a higher contribution of cargo traffic, compared to ports with a more mixed passenger-cargo traffic composition.

Total population weighted exposure to O_3 levels is at similar levels across cities, with a city average value of 66.29 $\mu g/m^3$ for the baseline year. This value does not change significantly after considering implementation of S3 or S8, with slightly more pronounced reductions during the summer period for most of the cities. Shipping contribution is relatively small to total O_3 exposure levels compared to the other examined pollutants, accounting for 3 % for the baseline year, 2 % for S3 and 4 % for S8. Some interesting trends are revealed, as for most of the European ports, shipping has a negative contribution in 2018 indicating a VOC-limited regime, a trend that persists in 2050 under the S8 scenario and much less under the S3 scenario, in some cases switching to a positive contribution. On the other hand, shipping contributes positively to the 2018 and 2050 O_3 concentrations in many North African and Middle Eastern ports, indicating a NO_x-limited regime in these areas. The highest shipping related O_3 exposures are calculated in Alexandria (5.84 $\mu g/m^3$) and Gaza (4.24 $\mu g/m^3$), followed by Port Said, Malta and Algiers at a value of ~4 $\mu g/m^3$ (Fig. 13).

Isolating the seasonal trends (Fig. 14) reveals that most of the negative contributions to O_3 concentrations are calculated in the winter months, while in the summer shipping has a consistent small positive contribution for all the cities.

3.4. Model validation results

The three regional models employed in the present study are widely used and extensively validated modelling tools, as described in section 2.2. As the scope of the study does not explicitly focus on model performance capabilities, the evaluation analysis performed considered the basic screening statistical indicators (mean bias - MB and fractional bias - FB), as suggested by the EPA. The equation used for the calculation of the FB indicator comparing observed (OB) and model predicted (PR) values is the following:

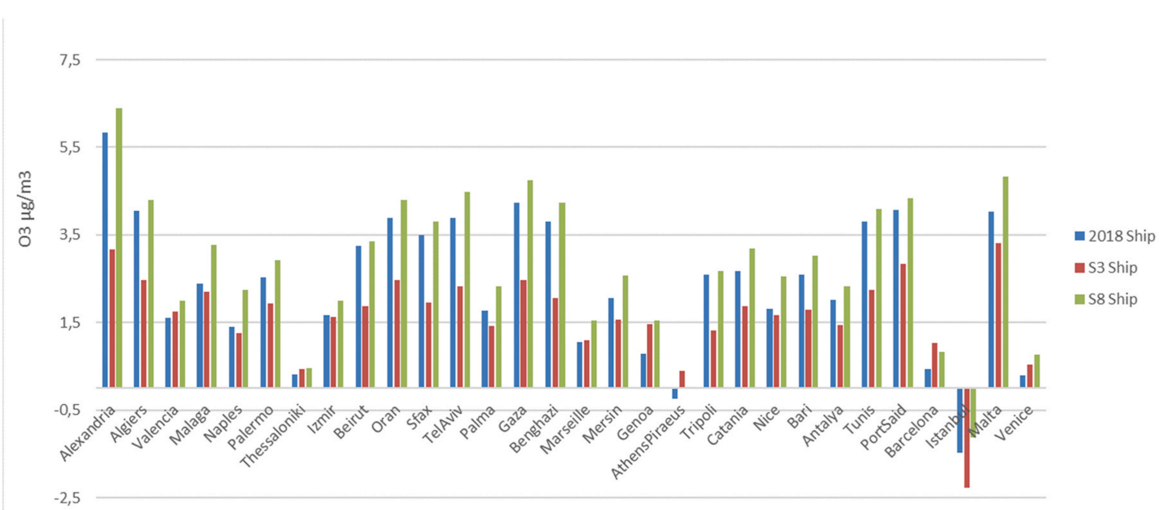

Fig. 13. Population weighted city exposures to shipping related O_3 ensemble annual concentrations for the baseline year and for S3 and S8.

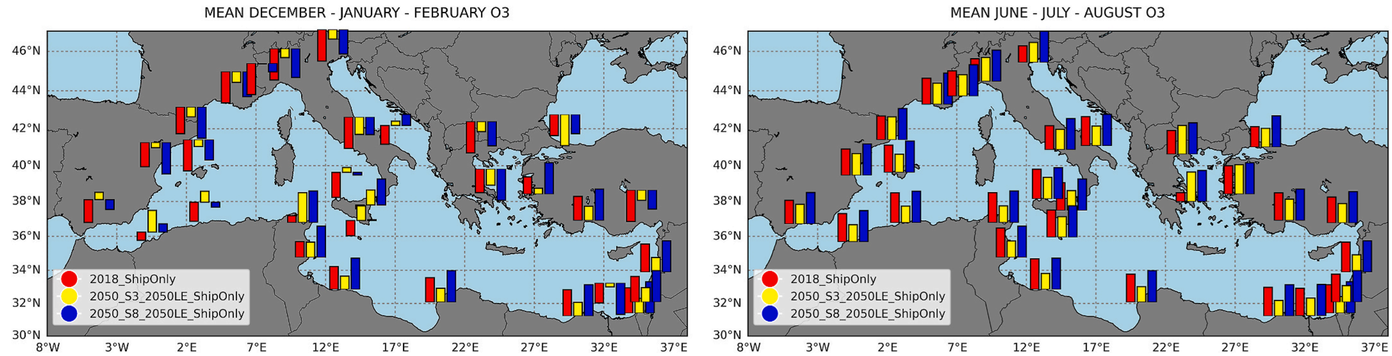

Fig. 14. Population weighted city exposures to shipping related O_3 ensemble winter (left) and summer (right) concentrations for the baseline year and for S3 and S8.

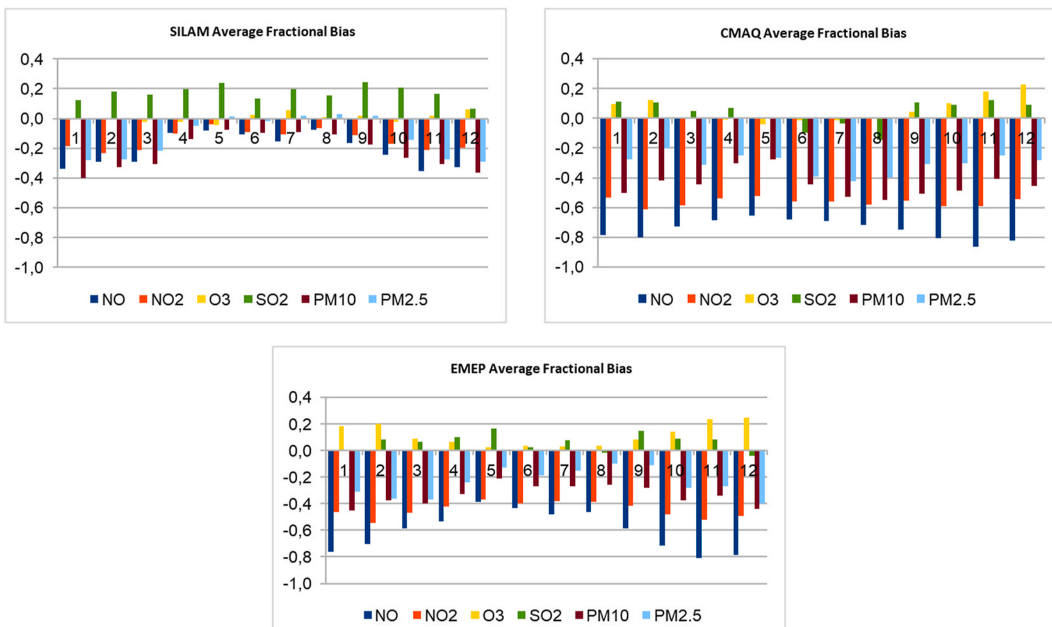

Fig. 15. Station average calculated Fractional Bias for the three dispersion models used.

$$FB = \frac{(OB - PR)}{(OB + PR)} \qquad \text{Equation 2}$$

The fractional bias is selected as a screening performance indicator, as it behaves symmetrically in terms of under- and overestimation, with values ranging between -1.0 (extreme overprediction) and $+1.0$ (extreme underprediction). In addition, the FB is represented by a dimensionless number which allows for comparing the results from different pollutants and concentration levels.

Data were extracted from AIRBASE for selected stations for all pollutants examined for 17 Mediterranean coastal cities (Malaga, Valencia, Barcelona, Marseille, Nice, Genova, Naples, Palermo, Malta, Catania, Bari, Piraeus, Thessaloniki, Istanbul, Izmir, Antalya, Mersin), where measurements of sufficient coverage for the baseline year were available. Measurements from urban or suburban/regional background monitoring stations were obtained to eliminate the influence of localized emission sources. In cases where the representative station for an examined city did not report measurements for all pollutants, an additional station was considered. To facilitate harmonization of reporting the evaluation results from the different models an excel form for automatically calculating the statistical indicators was developed and used.

Fig. 15 presents annual (2018) and monthly station average results for the Fractional Bias of the three individual models used for the ensemble calculations.

The validation results reveal certain differences in the models' behavior. There is a tendency of under-estimation of NO_x and PM_{10}, which is significant for EMEP and more pronounced for CMAQ but milder for SILAM, possibly due to its high resolution. In contrast to ozone, which is a secondary pollutant controlled by chemistry and photolysis, NO_x (especially NO) represent more local pollutants, which are sensitive to the quality of the emission inventory, the representativeness of observation stations and model resolution. For SILAM, the modelling performance of NO_x strongly benefits from its 5 km resolution, allowing higher urban levels to be modelled more accurately. This is seen in the smaller underestimation in the case of SILAM (FB ~ -0.2) than for EMEP and CMAQ. Same is also true to some extent for PM_{10}, which is also more local pollutant than ozone or $PM_{2.5}$. This representation error in SILAM is largest in winter, likely due to thinner boundary layer during the cold season and the even more localized emission impact. As mentioned previously, the strong negative bias in NO and NO_2, particularly in CMAQ (FB up to -0.8), may result from limitations in representing non-linear urban photochemistry. Additionally, the coarse model resolution (15 km) likely contributes to underestimations by failing to capture fine-scale spatial gradients near emission sources. Similar issues in simulating urban-scale reactive nitrogen species have been reported in recent CMAQ evaluations (Appel et al., 2012; Baker et al., 2023; She et al., 2024). EMEP model simulations performed on annual basis by MSC-W are regularly evaluated against measurement stations in EBAS; for 2022 also evaluation against the EEA monitoring stations is available (AeroVal - Evaluation, (Fagerli et al., 2024). Comparison with all EEA stations, including the urban and suburban stations, gives normalized mean biases for NO and NO2 -68 % and −38 % which are higher than for comparison with rural EEA stations (−49 % and −25 %) indicating larger bias for the urban and suburban stations likely caused by the above-mentioned causes.

SO_2 and O_3 predictions are satisfactory, with SO_2 modelled concentrations being overestimated but in a small extend, while O_3 modelled levels are slightly overestimated (with a monthly average FB value of 0.06 for CMAQ, 0.11 for EMEP and 0.005 for SILAM) as a result of underestimation of the ozone depleting NO_2. The model overestimation of measured O_3 is in agreement with results from relevant studies (Fink et al., 2023). More pronounced overestimation is observed during winter months (CMAQ, EMEP), possibly due to the chemical boundary conditions used in the regional models accounting for higher transported O_3 levels than locally produced in this period (Fink et al., 2023). For the urban stations EMEP demonstrates rather consistently higher O_3 concentrations with a corresponding underestimation of NO/NO_2. For the rural background station/stations, the model performs better. SILAM modelled SO_2 concentrations are more notably overestimated compared to the SO_2 calculated values of the CMAQ and EMEP models, however this bias does not correspond to lower predicted NO_2 levels. The overestimated CMAQ derived O_3 levels are more notable during the colder months, while in some cases during the warmer months, the model slightly underestimates O_3 concentrations. This behavior is also reported by Bravo et al. (Bravo et al., 2012) in their relevant study on the evaluation of CMAQ performance in relation to exposure estimation.

The higher negative FB values in the case of CMAQ and EMEP may reflect the coarse spatial resolution used for the simulations (15 km instead of 5 km in the case of SILAM), as regional scale results may fail in reproducing some urban features affecting pollutant dispersion or chemistry. For the purpose of this analysis, the higher resolution SILAM outputs were retained to preserve the added value of the finer resolution modelling in the ensemble output. Model estimations of reactive species participating in complex chemical reactions, such as PM and NOx, are characterized by a higher bias compared to SO_x calculations. This increased bias in the case of the reactive species may be associated with uncertainties in emissions, transport and vertical mixing model parameterizations. Another interesting finding is that FB values are reduced during the summer months for all models, particularly for SILAM and EMEP results. The monthly patterns of the station average FB are similar for the individual stations, with no notable inter-station variability observed for the results of all the three models. The seasonality in model bias may be related to the meteorological model performance producing the meteorological input variables. Zhang et al. (2013) in their long-term evaluation study of the WRF/CMAQ modelling system argued that water vapor content was reproduced well by WRF during spring, summer, and fall, but not during wintertime when significant biases and errors occurred which may influence particle formation. In spite of the biased predictions reported, the performance of the individual models is satisfactory overall with the annual mean FB (averaged for all stations) within the recommended performance criteria by Boylan and Russell (2006) of ±0.6.

4. Conclusions

An assessment of average annual and seasonal shipping contributions to atmospheric pollution levels over the Mediterranean region was performed under a baseline (2018) and two future emission reduction scenarios, using an ensemble modelling approach based on results of three chemical transport models (EMEP, SILAM, CMAQ).

The findings suggest that shipping NO_2 contributions are localised around routes and major ports with spatial maxima in the Gibraltar and Marmaras areas, amounting to about 95 % and 80 % of total concentrations for the two corresponding areas, while lesser local minima appear over water around the southern Mediterranean routes and major port areas. In land areas up to a few km off the Mediterranean coast the relative shipping impact ranges between 20 and 45 % of total NO_2 levels, with isolated peaks of about 50 % near the port hot-spots. Shipping contribution to O_3 concentrations can have a positive or negative sign, depending on the area background: positive contributions amount to about 9 % in a wide area around off-shore shipping routes with the effect gradually diminishing near coastlines, while a negative contribution of about −11 % is estimated near Gibraltar, along the main Aegean shipping route as well as close to major ports. The shipping contribution to $PM_{2.5}$ follows a similar spatial distribution to that of NO_2, with a spatial maximum of almost 50 % of total $PM_{2.5}$ in the western Mediterranean and near the Gibraltar strait, and a spatially smooth contribution amounting for between 10 % and 15 % over a strip along the coastline, extending a few km inland. Shipping has the dominating contribution to SO_2 concentrations along the major routes, with sharp maxima of about 93 % and 55 % over the Gibraltar strait and near the Istanbul port. Along the Mediterranean coast, shipping contributions amount from 40 % of total SO_2 off-coast down to about 25 % a few km inland.

In terms of the efficiency of emission reduction scenarios, the introduction of NECA reduces NO_2 shipping contributions by about 50 % along the main routes, while the alternative fuel scenario induces a much smaller reduction of about 12–15 %. Shipping has a positive contribution to O_3 near offshore shipping routes which becomes strongly negative near the hotspots. Both negative and positive contributions are largely reduced under the NECA scenario, while the alternative fuel scenario causes a smaller reduction leaving positive contributions very close to those of the 2018 baseline. Shipping contributions to $PM_{2.5}$ follow similar spatial distributions to that of NO_2, demonstrating a reduction of up to 85 % for the NECA and more than 90 % for the alternative fuel scenario. Restrictions under both 2050 scenarios are almost eliminating SO_2 shipping contributions by 90–95 % in most areas.

The findings of the present study reveal significant annual city average reductions of SO_2 and $PM_{2.5}$ shipping related exposure for both S3 (89.78 % reduction) and S8 (96.22 % reduction), while shipping induced NO_2 city-average exposure levels were efficiently controlled in S3 (42.74 %) but not in S8 (4.39 %).

The results of the present study provide a detailed and comprehensive insight into the impacts of shipping in the Mediterranean air quality under current and future high traffic growth shipping emission scenarios, based on quantified indicators calculated with the use of state-of-the-art and scientifically justified methodologies and tools. The findings suggest temporal and spatial variations in the effectiveness of the two scenarios studied, representing different abatement measures. It is important to note that this study is part of a wider integrated analysis exploring the impact of shipping emissions on the atmospheric and marine environment of the Mediterranean region, in some cases revealing contradicting effects. As S3 simulations indicate improvements in atmospheric quality and impairment of the marine water quality (due to increased discharge of scrubber effluent) and S8 produces the opposite results, a cost-benefit analysis approach before scenario implementation is recommended. The above findings can be employed to enable assessments of air quality and to evaluate the effectiveness of pollution control strategies in support to regional air quality management efforts. Looking beyond annual exposure, a more detailed estimate of shipping contributions taking into account temporal variations could benefit from calculating ensemble means weighted according to the uncertainty of each individual model. In this way, a more reliable estimate of contributions, including e.g. seasonal or acute exposures, could be obtained for supporting emissions policy and regulation enforcement.

CRediT authorship contribution statement

Evangelia Fragkou: Writing – review & editing, Writing – original draft, Validation, Project administration, Methodology, Formal analysis, Conceptualization. **George Tsegas:** Writing – review & editing, Writing – original draft, Visualization, Validation, Software, Methodology, Investigation, Formal analysis, Data curation. **Ummugulsum Alyuz:** Writing – original draft, Visualization, Validation, Software, Methodology, Formal analysis, Data curation. **Risto Hänninen:** Writing – original draft, Visualization, Validation, Software, Methodology, Investigation, Formal analysis, Data curation. **Jana Moldanova:** Writing – original draft, Visualization, Validation, Software, Methodology, Investigation, Formal analysis, Data curation. **Sara Jutterström:** Visualization, Validation, Software, Formal analysis, Data curation. **Elisa Majamäki:** Writing – original draft, Visualization, Validation, Software, Methodology, Formal analysis, Data curation. **Jukka-Pekka Jalkanen:** Writing – original draft, Project administration, Methodology, Investigation, Funding acquisition, Formal analysis, Data curation, Conceptualization. **Ranjeet S. Sokhi:** Writing – original draft, Supervision, Resources, Methodology, Investigation, Conceptualization. **Jaakko Kukkonen:** Writing – original draft, Supervision, Resources, Project administration, Methodology, Investigation, Funding acquisition, Conceptualization. **Mikhail Sofiev:** Supervision, Software, Resources, Methodology, Investigation, Conceptualization. **Leonidas Ntziachristos:** Supervision, Resources, Project administration, Methodology, Investigation, Funding acquisition, Conceptualization.

Declaration of competing interest

The authors declare that they have no known competing financial interests or personal relationships that could have appeared to influence the work reported in this paper.

Acknowledgements

This project has received funding from the European Union's Horizon 2020 research and innovation program under grant agreement No 874990 (EMERGE project). This work reflects only the authors' view and the Innovation and European Climate, Infrastructure and Environment Executive Agency (CINEA) is not responsible for any use that may be made of the information it contains. The authors are grateful to Mr. Panagiotis Gkirmpas for producing the figures for seasonal exposures to shipping emitted NO_2 and O_3. The authors wish to thank all members of EMERGE WP5 team for the scientific discussions in preparation of the EMERGE D6.2 Deliverable on the Mediterranean Sea Report on which this paper was based.

Appendix

Table A.1
Overview of the scenarios regarding the development of shipping in the future in the EMERGE project.

Scenario number	Ship traffic development	Number of scrubbers	SCRs in use	Low sulfur required	Ambition to reduce GHG emissions	Alternative fuels
1	High growth	High	NECA	SECA	No ambition	
2	High growth	High	NECA	SECA	No ambition	
3	High growth	High	Everywhere	Everywhere	No ambition	
4	Low growth	High	NECA	SECA	No ambition	LNG
5	Low growth	No scrubbers	None	SECA	50 % reduction	Methanol
6	High growth	High	NECA	SECA	50 % reduction	Methanol
7	High growth	Low	None	SECA	50 % reduction	Methanol
8	High growth	No scrubbers	None	SECA	50 % reduction	LNG & Methanol

Table A.2
Simulated transport work by shipping in the Mediterranean Sea in baseline year 2018 and the two scenarios in 2050.

	2018	2050 scenario 3	2050 scenario 8
Number of ships	18000	95000	95000
Transport work [km*ton]	7.68E+12	1.68E+13	1.68E+13
Number of ships with SCR	<10	92000	<10

Table A.3
Simulated ship fuel consumption in the Mediterranean Sea in 2018 and the two scenarios in 2050.

	2018	2050 scenario 3	2050 scenario 8
MGO [kg]	6.78E+08	7.05E+09	5.19E+09
MDO [kg]	2.68E+09	3.74E+09	1.64E+08
HFO [kg]	1.73E+10	1.83E+10	0.00E+00
Methane [kg]	1.73E+08	2.01E+08	4.90E+09
Methanol [kg]	n/a	0.00E+00	3.65E+10

Table A.4
Simulated ship emissions in the Mediterranean Sea in baseline year 2018 and the two scenarios in 2050.

	2018	2050 scenario 3	2050 scenario 8
PNC [1012]	1.02E+15	1.30E+15	3.59E+14
NOx [kg]	1.28E+09	3.99E+08	1.07E+09
SOx [kg]	7.61E+08	5.84E+07	1.62E+07
PM2.5 [kg]	7.64E+07	2.29E+07	6.60E+06
CO [kg]	9.07E+07	1.34E+08	5.63E+08
CO2 [kg]	6.61E+10	9.30E+10	8.38E+10
OC [kg]	2.46E+07	1.16E+07	5.21E+06
EC [kg]	2.29E+06	9.72E+05	3.75E+05
Ash [kg]	7.12E+06	1.49E+06	1.50E+05
SO4 [kg]	4.24E+07	8.85E+06	8.68E+05
CH4 [kg]	6.61E+06	6.52E+06	1.57E+08
NH3 [kg]	n/a	1.34E+07	0.00E+00
N2O [kg]	n/a	4.83E+06	1.88E+06
NMVOC [kg]	1.27E+07	1.84E+07	1.82E+07

Data availability

Tsegas, George (2024), "EMERGE Mediterranean Analysis", Mendeley Data, V1, doi: 10.17632/j56rgjsvz8.1

References

Aakko-Saksa, P.T., Lehtoranta, K., Kuittinen, N., Järvinen, A., Jalkanen, J.-P., Johnson, K., Jung, H., Ntziachristos, L., Gagné, S., Takahashi, C., Karjalainen, P., Rönkkö, T., Timonen, H., 2023. Reduction in greenhouse gas and other emissions from ship engines: current trends and future options. Prog. Energy Combust. Sci. 94, 101055. https://doi.org/10.1016/j.pecs.2022.101055.

Appel, K.W., Chemel, C., Roselle, S.J., Francis, X.V., Hu, R.-M., Sokhi, R.S., Rao, S.T., Galmarini, S., 2012. Examination of the community multiscale air quality (CMAQ) model performance over the North American and European domains. Atmos. Environ. 53, 142–155. https://doi.org/10.1016/j.atmosenv.2011.11.016.

Baker, K.R., Liljegren, J., Valin, L., Judd, L., Szykman, J., Millet, D.B., Czarnetzki, A., Whitehill, A., Murphy, B., Stanier, C., 2023. Photochemical model representation of ozone and precursors during the 2017 lake Michigan ozone study (LMOS). Atmos. Environ. 293, 119465. https://doi.org/10.1016/j.atmosenv.2022.119465.

Binkowski, F.S., Shankar, U., 1995. The regional particulate matter model. 1. Model description and preliminary results. Journal Of Geophysical Research-Atmospheres 100 (D12), 26191–26209.

Boylan, J.W., Russell, A.G., 2006. PM and light extinction model performance metrics, goals, and criteria for three-dimensional air quality models. Atmos. Environ. 40, 4946–4959. https://doi.org/10.1016/j.atmosenv.2005.09.087.

Bravo, M.A., Fuentes, M., Zhang, Y., Burr, M.J., Bell, M.L., 2012. Comparison of exposure estimation methods for air pollutants: Ambient monitoring data and regional air quality simulation, Environmental Research, Volume 116, 2012, Pages 1-10, ISSN 0013-9351.

DNV-GL, 2019. Energy Transition Outlook 2019, Maritime Forecast to 2050 Report.

DNV-GL, 2020. Energy Transition Outlook 2020, Maritime Forecast to 2050 Report.

Durán-Grados, V., Rodríguez-Moreno, R., Calderay-Cayetano, F., Amado-Sánchez, Y., Pájaro-Velázquez, E., Nunes, R.A.O., Alvim-Ferraz, M.C.M., Sousa, S.I.V., Moreno-Gutiérrez, J., 2022. The influence of emissions from maritime transport on air quality in the strait of Gibraltar (Spain). Sustainability 14 (19), 12507. https://doi.org/10.3390/su141912507.

Fagerli, H., et al., 2024. EMEP Status Report 1/2024, Transboundary Particulate Matter, photo-oxidants, Acidifying and Eutrophying Components. Norwegian Meteorological Institute emep.int/publ/reports/2024/EMEP_Status_Report_1_2024.pdf.

Fink, L., Karl, M., Matthias, V., Oppo, S., Kranenburg, R., Kuenen, J., Moldanova, J., Jutterström, S., Jalkanen, J.-P., Majamäki, E., 2023. Potential impact of shipping on air pollution in the Mediterranean region – a multimodel evaluation: comparison of photooxidants NO_2 and O_3. Atmos. Chem. Phys. 23, 1825–1862. https://doi.org/10.5194/acp-23-1825-2023.

Grigoriadis, A., Kousias, N., Raptopoulos-Chatzistefanou, A., Håkan, S., Moldanova, J., Lunde Hermansson, A., Cha, Y., Kontses, A., Toumasatos, Z., Mamarikas, S., Ntziachristos, L., 2024. Particulate and gaseous emissions from a large two-stroke slow-speed marine engine equipped with open-loop scrubber under real sailing conditions. Atmosphere 15, 845. https://doi.org/10.3390/atmos15070845.

Guenther, A., 2024. MEGANv2.1 code, user guide, input files, global BVOC emissions output, test case. Zenodo. https://doi.org/10.5281/zenodo.10525127.

Höglund-Isaksson, L., Gómez-Sanabria, A., Klimont, Z., Rafaj, P., Schöpp, W., 2020. Technical potentials and costs for reducing global anthropogenic methane emissions in the 2050 timeframe –results from the GAINS model. Environ. Res. Commun. 2 (2), 025004.

Jalkanen, J.-P., Brink, A., Kalli, J., Pettersson, H., Kukkonen, J., Stipa, T., 2009. A modelling system for the exhaust emissions of marine traffic and its application in the Baltic Sea area. Atmos. Chem. Phys. 9, 9209–9223. https://doi.org/10.5194/acp-9-9209-2009.

Jalkanen, J.-P., Johansson, L., Kukkonen, J., Brink, A., Kalli, J., Stipa, T., 2012. Extension of an assessment model of ship traffic exhaust emissions for particulate matter and carbon monoxide. Atmos. Chem. Phys. 12. https://doi.org/10.5194/acp-12-2641-2012.

Jalkanen, J.P., Johansson, L., Wilewska-Bien, M., Granhag, L., Ytreberg, E., Eriksson, K. M., Yngsell, D., Hassellöv, I.M., Magnusson, K., Raudsepp, U., Maljutenko, I., Winnes, H., Moldanova, J., 2021. Modelling of discharges from Baltic sea shipping. Ocean Sci. 17, 699–728. https://doi.org/10.5194/os-17-699-2021.

Jang, E., Choi, S., Yoo, E., Hyun, S., An, J., 2023. Impact of shipping emissions regulation on urban aerosol composition changes revealed by receptor and numerical modelling. npj Climate and Atmospheric Science 6, 52. https://doi.org/10.1038/s41612-023-00364-9.

Johansson, L., Jalkanen, J.-P., Kukkonen, J., 2017. Global assessment of shipping emissions in 2015 on a high spatial and temporal resolution. Atmos. Environ. 167, 403–415. https://doi.org/10.1016/j.atmosenv.2017.08.042.

Klimont, Z., Kupiainen, K., Heyes, C., Purohit, P., Cofala, J., Rafaj, P., Borken-Kleefeld, J., Schöpp, W., 2017. Global anthropogenic emissions of particulate matter including black carbon. Atmos. Chem. Phys. 17 (14), 8681–8723.

Kristensen, H.O., 2012. Energy demand and exhaust gas emissions of ships. Work Package 2 of Project Emissionsbeslutningsstøttesystem. Technical University of Denmark, Copenhagen.

Kuenen, J., Dellaert, S., Visschedijk, A., Jalkanen, J.-P., Super, I., Denier van der Gon, H., 2022. CAMS-REG-v4: a state-of-the-art high-resolution European emission inventory for air quality modelling. Earth Syst. Sci. Data 14, 491–515. https://doi.org/10.5194/essd-14-491-2022.

Luecken, D.J., Yarwood, G., Hutzell, W.H., 2019. Multipollutant modelling of ozone, reactive nitrogen, and HAPs across the continental US with CMAQ-CB6. Atmos. Environ. 201, 62–72. https://doi.org/10.1016/j.atmosenv.2018.11.060.

Maragkidou, A., Grönholm, T., Rautiainen, L., Nikmo, J., Jalkanen, J.-P., Mäkelä, T., Anttila, T., Laakso, L., Kukkonen, J., 2024. Measurement report: the effects of SECA regulations on the atmospheric SO 2 concentrations in the Baltic Sea, based on long-term observations at the Finnish Utö Island.

Merico, E., Gambaro, A., Argiriou, A., Alebic-Juretic, A., Barbaro, E., Cesari, D., Chasapidis, L., Dimopoulos, S., Dinoi, A., Donateo, A., Giannaros, C., Gregoris, E., Karagiannidis, A., Konstandopoulos, A.G., Ivošević, T., Liora, N., Melas, D., Mifka, B., Orlić, I., Poupkou, A., Sarovic, K., Tsakis, A., Giua, R., Pastore, T., Nocioni, A., Contini, D., 2017. Atmospheric impact of ship traffic in four Adriatic-Ionian port-cities: Comparison and harmonization of different approaches. Transportation Research Part D: Transport and Environment 50, 431–445. ISSN. https://doi.org/10.1016/j.trd.2016.11.016.

Mueller, N., Westerby, M., Nieuwenhuijsen, M., 2023. Health impact assessments of shipping and port-sourced air pollution on a global scale: A scoping literature review. Environ Res. 2023 Jan 1;216(Pt 1):114460. doi: 10.1016/j.envres.2022.114460. Epub 2022 Sep 30. PMID: 36191619.

Otte, T.L., Pleim, J.E., 2010. The Meteorology-Chemistry Interface Processor (MCIP) for the CMAQ modeling system: updates through MCIPv3.4.1. Geosci. Model Dev. (GMD) 3, 243–256. https://doi.org/10.5194/gmd-3-243-2010.

Schembari, C., Cavalli, F., Cuccia, E., Hjorth, J., Calzolai, G., Pérez, N., Pey, J., Prati, P., Raes, F., 2012. Impact of a European directive on ship emissions on air quality in Mediterranean harbours. Atmos. Environ. 61, 661–669. https://doi.org/10.1016/j.atmosenv.2012.06.047.

She, Y., Li, J., Lyu, X., Guo, H., Qin, M., Xie, X., Gong, K., Ye, F., Mao, J., Huang, L., Hu, J., 2024. Current status of model predictions of volatile organic compounds and impacts on surface ozone predictions during summer in China. Atmos. Chem. Phys. 24, 219–233. https://doi.org/10.5194/acp-24-219-2024.

Simpson, D., Benedictow, A., Berge, H., Bergstrom, R., Emberson, L.D., Fagerli, H., Flechard, C.R., Hayman, G.D., Gauss, M., Jonson, J.E., Jenkin, M.E., Nyiri, A., Richter, C., Semeena, V.S., Tsyro, S., Tuovinen, J.P., Valdebenito, A., Wind, P., 2012.

The EMEP MSC-W chemical transport model - technical description. Atmos. Chem. Phys. 12 (16), 7825–7865.
Simpson, D., Bergstrom, R., Briolat, A., Imhof, H., Johansson, J., Priestley, M., Valdebenito, A., 2020. GenChem v1.0-a chemical pre-processing and testing system for atmospheric modelling. Geosci. Model Dev. (GMD) 13 (12), 6447–6465.
Skamarock, W.C., Klemp, J.B., Dudhia, J., Gill, D.O., Liu, Z., Berner, J., Wang, W., Powers, J.G., Duda, M.G., Barker, D.M., Huang, X.-Y., 2019. A description of the advanced research WRF version 4. NCAR Tech. Note NCAR/TN-556+STR 145. https://doi.org/10.5065/1dfh-6p97.
Smith, T.W.P., Jalkanen, J.-P., Anderson, B.A., Corbett, J.J., Faber, J., Hanayama, S., O'Keeffe, E., Parker, S., Johansson, L., Aldous, L., Raucci, C., Traut, M., Ettinger, S., Nelissen, D., Lee, D.S., Ng, S., Agrawal, A., Winebrake, J.J., Hoen, M., Chesworth, S., Pandey, A., 2015. Third IMO GHG Study 2014. International Maritime Organization (IMO), london, UK. April 2015.
The institute for the Environment - The University of North Carolina at Chapel Hill, 2018. SMOKE v4.6 User's Manual.
Toscano, D., 2023. The impact of shipping on air quality in the port cities of the Mediterranean Area: a review. Atmosphere 14, 1180. https://doi.org/10.3390/atmos14071180.
US EPA, 2020. CMAQ (Version 5.3.2) [Software].
US EPA, 2021. EQUATESv1.0: emissions, WRF/MCIP, CMAQv5.3.2 data – 2002-2019 US_12km and NHEMI_108km. UNC Dataverse. https://doi.org/10.15139/S3/F2KJSK. V5.
Vautard, R., Schaap, M., Bergström, R., Bessagnet, B., Brandt, J., Builtjes, P.J.H., Christensen, J.H., Cuvelier, C., Foltescu, V., Graff, A., Kerschbaumer, A., Krol, M., Roberts, P., Rouïl, L., Stern, R., Tarrason, L., Thunis, P., Vignati, E., Wind, P., 2009. Skill and uncertainty of a regional air quality model ensemble. Atmos. Environ. 43 (31), 4822–4832. https://doi.org/10.1016/j.atmosenv.2008.09.083.
Viana, M., Hammingh, P., Colette, A., Querol, X., Degraeuwe, B., de Vlieger, Ina, van Aardenne, John, 2014. Impact of maritime transport emissions on coastal air quality in Europe. Atmos. Environ. 90, 96–105. https://doi.org/10.1016/j.atmosenv.2014.03.046.
Viana, M., Rizza, V., Tobías, A., Carr, E., Corbett, J., Sofiev, M., Karanasiou, A., Buonanno, G., Fann, N., 2020. Estimated health impacts from maritime transport in the Mediterranean region and benefits from the use of cleaner fuels. Environ. Int. 138, 105670. https://doi.org/10.1016/j.envint.2020.105670.
Yarwood, G., Yocke, S.R.M., Whitten, G., 2005. Updates to the Carbon Bond Mechanism: CB05. U.S. Environmental Protection Agency, p. 161. Final Report.
Zhang, Y., Sartelet, K., Wu, S.-Y., Seigneur, C., 2013. Application of WRF/Chem-MADRID and WRF/Polyphemus in Europe – part 1: model description, evaluation of meteorological predictions, and aerosol–meteorology interactions. Atmos. Chem. Phys. 13 (14), 6807–6843. https://doi.org/10.5194/acp-13-6807-2013.